

Stress Analysis in Longwall Entry Roof Under High Horizontal Stress

by

Hanjie Chen

A Dissertation

Submitted to

Department of Mining Engineering
College of Engineering and Mineral Resources
West Virginia University

In Partial Fulfillment of the Requirements

For the Degree of

Doctor of Philosophy

In

Mining Engineering

Syd S. Peng, Ph.D., Chairman

Abdul W. Khair, Ph.D.

Bruce Kang, Ph.D.

Yi Luo, Ph.D.

Christopher Mark, Ph.D.

Morgantown, West Virginia

1999

Keyword: Horizontal Stress, Longwall Mining, Stress Angle, Interface Sliding

Copyright 1999 Hanjie Chen

Stress Analysis in Longwall Entry Roof Under High Horizontal Stress

by
Hanjie Chen

ABSTRACT

High horizontal stress plays an important role in ground control in longwall mining. It can significantly affect the stability of the panel entry system in both the development and mining periods. Many roof problems have been contributed to high horizontal stress, especially when the immediate roof is weak, or thinly bedded.

In this research, the stress distributions in the entry roof in longwall mining have been studied when the high horizontal stress occurs. Using a three-dimensional finite element method, the stresses in the entry roof have been analyzed for the different cases. It is found that the stress angle is the most important factor that affects the roof stability when the magnitude of horizontal stress is fixed. Generally, the longwall entries are in the worst stress conditions when the stress angle is about $60^{\circ} \sim 75^{\circ}$.

At the T-junctions of a longwall panel, the entries are subjected to large front abutment pressure. Under horizontal stress, the roof stresses at the T-junctions increase with the stress angle. In a single panel, the stress in the headgate entries is larger than that in the tailgate entries when the maximum horizontal stress is from the headgate side. In a multiple-panel system, the stress in the headgate is larger when the horizontal stress is from the gob side than that from the solid coal side. But, the stress in the tailgate is always larger than that in the headgate.

Roof failures often occur in the laminated roof, where the roof consists of some rock layers. In this situation, the slip between the coal seam and the roof/floor may occur. In addition, the roof separations can appear. In this study, the roof separations and the slip have been simulated. Because of the slip between the coal seam and the roof/floor, the stresses in

the entry roof relieve to some degree. If the coefficient of friction in the interfaces is small, the stresses in the roof relieve significantly. The stresses in the roof increase with the coefficient of friction and the stress ratio of the horizontal to the vertical stress. When the roof separations occur, the stresses in the roof increase. Usually, the lowest roof layer is subjected to the largest loading. On the upper surface of this layer, tensile stress occurs along the vertical direction, which will worsen the roof condition.

ACKNOWLEDGEMENTS

The author wishes to express his sincere appreciation and gratitude to those who have contributed to the preparation and completion of this dissertation. With respect and gratitude, the author is deeply indebted to all members of his advisory and examination committee: Dr. Abdul W. Khair, Dr. Bruce Kang, Dr. Yi Luo, and Dr. Christopher Mark for their supports and invaluable suggestions during this research work. Their guidance, concern, and positive thinking will long be remembered and appreciated.

Sincere gratitude and appreciation is expressed to Dr. Syd S. Peng, Chairman of the advisory and examination committee, for initially suggesting the problem, and for his supervision, interest, and interesting discussions provided throughout this study. His guidance has been invaluable to the completion of this dissertation.

The author also wishes to express his thanks to his fellow students and staffs of COMER for their help.

Finally, the author expresses his sincere thanks to his wife, Zhen Lu, and his daughter, Haoqian, whose patience, support and loving make the completion of the dissertation especially fruitful.

TABLE OF CONTENTS

ABSTRACT	(ii)
ACKNOWLEDGEMENTS	(iv)
LIST OF TABLES	(v)
LIST OF FIGURES	(ix)
LIST OF SYMBOLS	(xvii)
1. INTRODUCTION	(1)
2. LITERATURE REVIEW	(3)
2.1 Horizontal Stress in US Coal Fields	(4)
2.2 Cutter Roof Failure	(7)
2.3 Influence of Horizontal Stress on Longwall Mining	(14)
2.4 Remarks on Previous Studies	(21)
3. RESEARCH SCOPE AND INITIAL STUDY	(22)
3.1 Introduction	(22)
3.2 Research Scope	(22)
3.3 Selection of the Method of Analysis	(29)
3.4 Mechanics of Roof Failure	(29)
3.5 Initial Study	(35)
4. ROOF STRESS DURING ENTRY DEVELOPMENT	(52)
4.1 General Consideration	(52)
4.2 Roof Stress without Horizontal Stress	(55)
4.3 Influence of Stress Angle on Roof Stress	(60)
4.4 Influence of Stress Ratio on Roof Stress	(100)
4.5 Von-Mises Stress in Higher Horizontal Stress Field	(106)
4.6 Stress in Medium Immediate Roof	(109)
4.7 Sequence of Entry Development	(111)

4.8 Discussion of Results	(115)
5. ROOF STRESS IN LONGWALL PANELS	(127)
5.1 Introduction	(127)
5.2 Finite Element Models	(128)
5.3 Stress in Entry Roof in a Single Panel	(134)
5.4 Stress in Entry Roof in a Multiple-panel System	(170)
5.5 Discussion of Results	(195)
6. ROOF STRESS WITH INTERFACE SLIDING BETWEEN LAYERS	(202)
6.1 Introduction	(202)
6.2 Research Scope and Methods	(205)
6.3 Roof Stress with Interfaces between Coal and Roof/Floor	(208)
6.4 Roof Stress with Interfaces between Layers	(226)
6.5 Discussion of Results	(250)
7. CONCLUSIONS AND RECOMMENDATIONS	(267)
7.1 Conclusions	(267)
7.2 Recommendations for Panel Design and Entry Roof Support	(272)
REFERENCES	(274)
VITA	(278)

LIST OF TABLES

<u>Table</u>	<u>Page</u>
Table 2-1 Results of Minifrac Stress Measurements in Southwestern PA and Northern WV	(6)
Table 2-2 Horizontal Components of in-situ Stress at Six West Virginia Mines	(7)
Table 2-3 Induced Von-Mises Stress Concentration in the Headgate Roof	(18)
Table 2-4 The Maximum Stress Concentration Factor (SCF)	(19)
Table 3-1 Geological Conditions in Some Roof Failure Areas	(26)
Table 3-2 Mises Stresses in the Combinations of the Main Factors	(46)
Table 3-3 Min. Principal Stresses in the Combinations of the Main Factors	(47)
Table 4-1 Rock Properties Used in The Study	(53)
Table 4-2 Stresses at Points for Different Angles in Entry 1	(86)
Table 4-3 Stresses at Points for Different Angles in Entry 2	(87)
Table 4-4 Stresses at Points for Different Angles in Entry 3	(88)
Table 4-5 Stresses at Points in Crosscuts 1 and 2	(99)
Table 4-6 Von-Mises Stress Change with the Ratio in Entry 1	(102)
Table 4-7 Von-Mises Stress Change with the Ratio in Entry 2	(102)
Table 4-8 Von-Mises Stress Change with the Ratio in Entry 3	(104)
Table 4-9 Von-Mises Stresses for Different Horizontal Stresses	(107)
Table 4-10 Von-Mises Stresses in Different types of Roof	(109)
Table 5-1 Reduction Factors for Gob Materials	(129)
Table 6-1 Rock Properties Used in The Study	(206)
Table 6-2 Coefficients of Friction Used in The Study	(226)
Table 6-3 Von-Mises Stress Near Rib Side	(251)
Table 6-4 Max. Principal Stress Near Rib Side	(252)
Table 6-5 Orientations of Max. Principal Stress Near Rib Side (degree)	(253)
Table 6-6 Min. Principal Stress Near Rib Side	(256)
Table 6-7 Stress along Horizontal direction Near Rib Side	(257)

<u>Table</u>	<u>Page</u>
Table 6-8 Von-Mises Stress at Points P1 and P2	(259)
Table 6-9 Max. Principal Stress at Points P1 and P2	(261)
Table 6-10 Orientations of Max. Principal Stress at Points P1 and P2 (degree)	(263)
Table 6-11 Min. Principal Stress at Points P1 and P2	(265)
Table 6-12 Stress along Horizontal Stress at Points P1 and P2	(266)

LIST OF FIGURES

<u>Figure</u>	<u>Page</u>
Fig. 2-1 Orientation of the Maximum Horizontal Stress in Deep Boreholes	(5)
Fig. 2-2 Orientation of the Max. Horizontal Stress Measured In Eastern US Coal Mines	(5)
Fig. 2-3 Stress Provinces of the Continental United States	(6)
Fig. 2-4 Regional Horizontal Stress Fields and Locations of Mines	(7)
Fig. 2-5 Typical Cutter Roof Failure at Entry Corner	(8)
Fig. 2-6 Remaining Cavity Following Overall Roof Collapse	(8)
Fig. 2-7 Progressive Sequence of Events Leading to Overall Roof Collapse Resulting from Cutter Roof Failure	(9)
Fig. 2-8 Layout of Study Site in Beth Energy Mines	(10)
Fig. 2-9 Cutter Roof Develops a Short Distance behind the Face and Follows Entry Advance	(11)
Fig. 2-10 Failed Roof Bolt at the Cutter Zone	(11)
Fig. 2-11 Longwall Projections	(13)
Fig. 2-12 Cutter Roof in Longwall Development Entries	(13)
Fig. 2-13 Roof Condition in Different Mining Directions	(15)
Fig. 2-14 Horizontal Stress Concentration Caused by Retreat Mining	(16)
Fig. 2-15 The Study Site in Mines A and B	(17)
Fig. 2-16 Relative Orientation of Max. Horizontal Stress and Direction of Mining	(18)
Fig. 2-17 Finite Element Models Used by Peng and Wang	(19)
Fig. 2-18 Roof Failure vs. Stress Angle	(20)
Fig. 2-19 Effect of Horizontal Stress Direction	(20)
Fig. 3-1 The Geological Conditions Used in the Models	(23)
Fig. 3-2 Finite Element Models (Plan View)	(27)
Fig. 3-3 Sequence of Cutting in Entry Development	(28)

<u>Figure</u>	<u>Page</u>
Fig. 3-4 Possible Forms of Roof Failure	(30)
Fig. 3-5 Mechanical Model for Roof Failure	(31)
Fig. 3-6 Sliding Between Layers under Lateral Stress	(32)
Fig. 3-7 Strong Roof Under High Horizontal Stress	(32)
Fig. 3-8 Combinations of Main Factors Considered in the Study	(37)
Fig. 3-9 Plan View of 3-D Models for Initial Study	(36)
Fig. 3-10 Stress Distributions in Immediate Roof without Horizontal Stress	(40)
Fig. 3-11 Stress Distributions in Immediate Roof with Horizontal Stress	(41)
Fig. 3-12 Mises Stress Changes in Immediate Roof with the Angle	(45)
Fig. 3-13 Mises Stress Distributions in Immediate Roof with Different Overburdens	(48)
Fig. 3-14 Min. Principal Stress Distributions in Immediate Roof with Different Overburdens	(49)
Fig. 3-15 Von-Mises Stress Changes with the Stress Ratio	(50)
Fig. 3-16 Von-Mises Stress distributions in the Different Types of Immediate Roof	(51)
Fig. 4-1 Typical 3-D Models for Entry development	(54)
Fig. 4-2 Von Mises Stress in Entry Roof without Horizontal Stress	(57)
Fig. 4-3 Max. Principal Stress in Entry Roof without Horizontal Stress	(58)
Fig. 4-4 Min. Principal Stress in Entry Roof without Horizontal Stress	(59)
Fig. 4-5 Locations of Measurement Lines and Points	(61)
Fig. 4-6 Von-Mises Stress Change with the Angle in Entry 1	(65)
Fig. 4-7 Von-Mises Stress Change with the Angle in Different Cross Sections of Entry 1	(66)
Fig. 4-8 Min. Principal Stress Change with the Angle in Different Cross Sections of Entry 1	(67)
Fig. 4-9 Max. Principal Stress Change with the Angle in Different Cross Sections of Entry 1	(68)
Fig. 4-10 Von-Mises Stress Change with the Stress Angle in Entry 2	(73)

<u>Figure</u>	<u>Page</u>
Fig. 4-11 Von-Mises Stress Change with the Angle in Different Cross Sections of Entry 2	(74)
Fig. 4-12 Min. Principal Stress Change with the Angle in Different Cross Sections of Entry 2	(75)
Fig. 4-13 Max. Principal Stress Change with the Angle in Different Cross Sections of Entry 2	(76)
Fig. 4-14 Von-Mises Stress Change with the Angle in Entry 3	(81)
Fig. 4-15 Von-Mises Stress Change with the Angle in Different Cross Sections of Entry 3	(82)
Fig. 4-16 Min. Principal Stress Change with the Angle in Different Cross Sections of Entry 3	(83)
Fig. 4-17 Max. Principal Stress Change with the Angle in Different Cross Sections of Entry 3	(84)
Fig. 4-18 The Locations of Lines, Cross Sections, and Points in Crosscuts 1 and 2	(92)
Fig. 4-19 Von-Mises Stress Change with the Angle in Crosscut 1	(93)
Fig. 4-20 Von-Mises Stress Change with the Angle in Crosscut 2	(94)
Fig. 4-21 Von-Mises Stress Change with the Angle in Different Cross Sections in Crosscut 1	(95)
Fig. 4-22 Von-Mises Stress Change with the Angle in Different Cross Sections in Crosscut 2	(96)
Fig. 4-23 Max. Principal Stress Change with the Angle in Different Cross Sections in Crosscut 1	(97)
Fig. 4-24 Max. Principal Stress Change with the Angle in Different Cross Sections in Crosscut 2	(98)
Fig. 4-25 Influence of the Stress Ratio on Von-Mises Stress in Entry 1	(101)
Fig. 4-26 Influence of the Stress Ratio on Von-Mises Stress for Different Angles in Entry 1	(101)
Fig. 4-27 Influence of the Stress Ratio on Von-Mises Stress in Entry 2	(103)

<u>Figure</u>	<u>Page</u>
Fig. 4-28 Influence of the Stress Ratio on Von-Mises Stress for Different Angles in Entry 2	(103)
Fig. 4-29 Influence of the Stress Ratio on Von-Mises Stress in Entry 3	(105)
Fig. 4-30 Influence of the Stress Ratio on Von-Mises Stress for Different Angles in Entry 3	(105)
Fig. 4-31 Von-Mises Stress Distribution in Entries ($\sigma_{h\max} = 4,500$ psi)	(107)
Fig. 4-32 Von-Mises Stress in Entries for Different Horizontal Stresses	(108)
Fig. 4-33 Von-Mises Stress Distributions in Different Types of Roof	(110)
Fig. 4-34 Von-Mises Stress Contours in Sequence of Entry Development	(113)
Fig. 4-35 Conceptual Explanation of Cutter Roof	(116)
Fig. 4-36 Von-Mises Stress Distribution in Entry Roof	(116)
Fig. 4-37 Typical Roof Stress Distributions in Entry 1	(121)
Fig. 4-38 Typical Roof Stress Distributions in Entry 2	(122)
Fig. 4-39 Typical Roof Stress Distributions in Entry 3	(123)
Fig. 4-40 Von-Mises Stress after Entry Development	(124)
Fig. 4-41 The Possible Locations of Cutter Roof	(125)
Fig. 4-42 Von-Mises Stress in Coal Seam around Entry 2	(126)
Fig. 4-43 Max. Principal Stress in Coal Seam around Entry 2	(126)
Fig. 5-1 Plan View of Basic Model for Single Panel and Locations of Lines	(130)
Fig. 5-2 Plan View of Basic Model for Multiple Panels and Locations of Lines	(131)
Fig. 5-3 Determination of Model Height	(132)
Fig. 5-4 Models and Meshes for Longwall Panels	(133)
Fig. 5-5 Stress Distributions at Roof Line Level in Headgate 1	(136)
Fig. 5-6 Stress Distributions at Roof Line Level in Headgate 2	(137)
Fig. 5-7 Stress Distributions at Roof Line Level in Headgate 3	(138)
Fig. 5-8 Von-Mises Stress in Headgate 1	(142)
Fig. 5-9 Von-Mises Stress at the Some Points in Headgate 1	(143)
Fig. 5-10 Max. Principal Stress in Headgate 1	(144)
Fig. 5-11 Max. Principal Stress at the Specified Points in Headgate 1	(145)

<u>Figure</u>	<u>Page</u>
Fig. 5-12 Min. Principal Stress in Headgate 1	(146)
Fig. 5-13 Min. Principal Stress at the Some Points in Headgate 1	(147)
Fig. 5-14 Von-Mises Stress in Tailgate 1	(150)
Fig. 5-15 Von-Mises Stress at the Some Points in Tailgate 1	(151)
Fig. 5-16 Max. Principal Stress in Tailgate 1	(152)
Fig. 5-17 Max. Principal Stress at the Some Points in Tailgate 1	(153)
Fig. 5-18 Min. Principal Stress in Tailgate 1	(154)
Fig. 5-19 Min. Principal Stress at the Some Points in Tailgate 1	(155)
Fig. 5-20 Comparisons of Stresses at the Two T-Junctions	(157)
Fig. 5-21 Von-Mises Stress in Headgate 2	(161)
Fig. 5-22 Von-Mises Stress at the Specified Points in Headgate 2	(162)
Fig. 5-23 Max. Principal Stress in Headgate 2	(163)
Fig. 5-24 Max. Principal Stress at the Specified Points in Headgate 2	(164)
Fig. 5-25 Von-Mises Stress in Tailgate 2	(165)
Fig. 5-26 Von-Mises Stress at the Specified Points in Tailgate 2	(166)
Fig. 5-27 Max. Principal Stress in Tailgate 2	(167)
Fig. 5-28 Max. Principal Stress at the Specified Points in Tailgate 2	(168)
Fig. 5-29 Comparisons of Von-Mises Stress at the Specified Points in Headgate 2 and Tailgate 2	(169)
Fig. 5-30 Von-Mises Stress in Headgate 1 (σ_{hmax} from Gob Side)	(172)
Fig. 5-31 Von-Mises Stress in Headgate 1 (σ_{hmax} from Solid Coal Side)	(173)
Fig. 5-32 Comparison of Von-Mises Stress in Headgate 1	(174)
Fig. 5-33 Von-Mises Stress in Tailgate 1 (σ_{hmax} from Gob Side)	(176)
Fig. 5-34 Von-Mises Stress in Tailgate 1 (σ_{hmax} from Solid Coal Side)	(177)
Fig. 5-35 Comparison of Von-Mises Stress in Tailgate 1	(178)
Fig. 5-36 Max. Principal Stress in Headgate 1 (σ_{hmax} from Gob Side)	(180)
Fig. 5-37 Max. Principal Stress in Headgate 1	(181)
Fig. 5-38 Comparison of Max. Principal Stress in Headgate 1	(182)
Fig. 5-39 Max. Principal Stress in Tailgate 1 (σ_{hmax} from Gob Side)	(184)

<u>Figure</u>	<u>Page</u>
Fig. 5-40 Max. Principal Stress in Tailgate 1	(185)
Fig. 5-41 Comparison of Max. Principal Stress in Tailgate 1	(186)
Fig. 5-42 Min. Principal Stress in Headgate 1 (σ_{hmax} from Gob Side)	(188)
Fig. 5-43 Min. Principal Stress in Headgate 1	(189)
Fig. 5-44 Min. Principal Stress in Tailgate 1 (σ_{hmax} from Gob Side)	(190)
Fig. 5-45 Min. Principal Stress in Tailgate 1	(191)
Fig. 5-46 Comparison of Von-Mises Stress Between Headgate and Tailgate	(193)
Fig. 5-47 Comparison of Max. Principal Stress Between Headgate and Tailgate	(194)
Fig. 5-48 Typical Stress Distributions at T-Junctions (P1)	(196)
Fig. 5-49 Typical Stress Distributions at T-Junctions (P3)	(197)
Fig. 5-50 Typical Stress Distributions at Headgate T-Junctions (P1)	(199)
Fig. 5-51 Typical Stress Distributions at Headgate T-Junctions (P3)	(200)
Fig. 5-52 Von-Mises Stress Distributions at Headgate T-Junction	(201)
Fig. 6-1 Strata Deformations without/with Sliding between Roof/Floor and Coal and between Roof Layers without Horizontal Stress	(203)
Fig. 6-2 Strata Deformations without/with Sliding between Roof/Floor and Coal and between Roof Layers with Horizontal Stress	(204)
Fig. 6-3 Finite Element Models	(207)
Fig. 6-4 Von-Mises Stress at the Roof Line Level (Level 1)	(211)
Fig. 6-5 Typical Von-Mises Stress with the Frictional Coefficient (R=3)	(212)
Fig. 6-6 Von-Mises Stress at Two Specified Points in the Roof For Different Stress Ratios (R=3~7)	(212)
Fig. 6-7 Von-Mises Stress at Different Levels in the Roof	(213)
Fig. 6-8 Typical Von-Mises Stress Distribution in the Roof For the Frictional Coefficient (R=5)	(214)
Fig. 6-9 Max. Principal Stress at the Roof Line Level	(216)
Fig. 6-10 Typical Max. Principal Stress Change at the Roof Line Level with Different Frictional Coefficients	(217)
Fig. 6-11 Max. Principal Stress at the Specified Points	(217)

<u>Figure</u>	<u>Page</u>
Fig. 6-12 Typical Max. Principal Stress Distribution at Different Levels	(218)
Fig. 6-13 Min. Principal Stress at the Roof Line Level	(220)
Fig. 6-14 Typical Min. Principal Stress Distributions at Different Roof Levels (R=5)	(221)
Fig. 6-15 Stress along the Horizontal Direction at the Roof Line Level	(223)
Fig. 6-16 Typical Distribution of the Stress along Horizontal Direction in the Roof (R=5)	(224)
Fig. 6-17 Vertical Displacements in the Different Roof Layers	(227)
Fig. 6-18 Von-Mises Stress in the Different Layers (R=3, $f_1=0.4$, $f_2=0.2$)	(230)
Fig. 6-19 Von-Mises Stress at the Roof Line level for Different Cases (R=3)	(231)
Fig. 6-20 Von-Mises Stress at the Roof Line level for Different Cases (R=5)	(232)
Fig. 6-21 Von-Mises Stress at the Roof Line level for Different Cases (R=7)	(232)
Fig. 6-22 Max. Principal Stress in the Different Layers (R=3, $f_1=0.4$, $f_2=0.2$)	(235)
Fig. 6-23 Max. Principal Stress at the Roof Line level for Different Cases (R=3)	(236)
Fig. 6-24 Max. Principal Stress at the Roof Line level for Different Cases (R=5)	(237)
Fig. 6-25 Max. Principal Stress at the Roof Line level for Different Cases (R=7)	(238)
Fig. 6-26 Min. Principal Stress in the Different Layers (R=3, $f_1=0.4$, $f_2=0.2$)	(241)
Fig. 6-27 Min. Principal Stress at the Roof Line Level (R=3)	(242)
Fig. 6-28 Min. Principal Stress at the Roof Line Level (R=5)	(243)
Fig. 6-29 Min. Principal Stress at the Roof Line Level (R=7)	(244)
Fig. 6-30 Stress along Horizontal Direction in the Different Layers	(246)
Fig. 6-31 Stress along Horizontal Direction at the Roof Line Level (R=3)	(247)
Fig. 6-32 Stress along Horizontal Direction at the Roof Line Level (R=5)	(248)
Fig. 6-33 Stress along Horizontal Direction at the Roof Line Level (R=7)	(249)
Fig. 6-34 Typical Von-Mises Stress at Roof Line Level	(251)
Fig. 6-35 Typical Max. Principal Stress at the Roof Line Level	(252)
Fig. 6-36 Orientation of the Max. Principal Stress with Interface Sliding	(254)
Fig. 6-37 Orientation of the Max. Principal Stress vs. Coefficient of Friction	(255)
Fig. 6-38 Direction of Roof Failure Plane	(255)

<u>Figure</u>	<u>Page</u>
Fig. 6-39 Typical Min. Principal Stress at the Roof Line Level	(256)
Fig. 6-40 Typical Stress along the Horizontal Direction	(257)
Fig. 6-41 Typical Von-Mises Stress in the First Roof Layer	(259)
Fig. 6-42 Typical Max. Principal Stress in the first Layer	(260)
Fig. 6-43 Orientation of the Max. Principal Stress (R=5, f1=0.4)	(261)
Fig. 6-44 Orientation of the Max. Principal Stress at One Rib Side	(262)
Fig. 6-45 Typical Min. Principal Stress in the First Layer	(264)
Fig. 6-46 Typical Vertical Stress in the First Layer	(264)
Fig. 6-47 Typical Stress along the Horizontal Direction in the First Layer	(265)
Fig. 7-1 Recommendation for Langwall Panel Design	(252)

LIST OF SYMBOLS

E	Young's Modulus
ν	Poisson' Ratio
$\sigma_1, \sigma_2, \sigma_3,$	Principal Stresses
σ_{VM}	Von-Mises Stress
σ_c	Unconfined Compressive Strength
σ_t	Unconfined Tensile Strength
σ_0	Tested Strength of Material
σ_n	Normal Stress on a Plane
τ	Shear Stress
τ_{max}	Maximum Shearing Stress
C	Cohesion of the Material
β	Internal Friction Angle of Material
σ_v	Applied Vertical Stress
σ_h	Horizontal Stress
σ_{hmax}	Applied Maximum Horizontal Stress
σ_{hmin}	Applied Minimum Horizontal Stress
α	Stress Angle between the Orientation of the Max. Horizontal Stress to the Entry Direction or the Mining Direction
R	Stress Ratio of Applied Max. Horizontal Stress to Applied Vertical Stress ($R = \sigma_{hmax} / \sigma_v$)
r	Stress Ratio of Applied Max. Horizontal Stress to Applied Min. Horizontal Stress ($r = \sigma_{hmax} / \sigma_{hmin}$)
f	Coefficient of Friction in the Interfaces
f_1	Coefficient of Friction in the Interfaces between Coal and Roof/Floor
f_2	Coefficient of Friction in the Interfaces between Roof Layers

CHAPTER 1

INTRODUCTION

In recent years, researchers have often attribute coal mine roof stability problems to high horizontal stress. High horizontal stress plays an important role in ground control in longwall mining. In longwall mines, high horizontal stress could cause cutter roof failure. It can significantly affect the stability of the panel entry system in both the development and mining periods. Underground observations have shown that in northeastern North America the maximum horizontal stress are usually greater than the minimum horizontal stress and that longwall entries nearly perpendicular to the maximum horizontal stress suffer greater damage than those oriented parallel to it.

However, it is still relatively unknown how the high horizontal stress influences the entry system in a multiple-panel system. Whether or not a previous mined-out panel can reduce the loading, and if so how much reduction, on the tailgate entry system of the immediately adjacent longwall panel. In addition, it is also a poorly understood how the ratio of the maximum horizontal stress to the minimum horizontal stress affects the longwall entry roof stability.

Since roof failure is more likely to occur in laminated weak roof subjected to high horizontal stress, it is thought that the roof consists of some layers and these layers may slide and separate. Field measurements have confirmed that separation often occurs in the laminated roof. In this situation, how the stress in the roof is redistributed is still unknown.

Therefore, it is necessary to study the mechanism of entry roof failure in longwall mining and to analyze the factors that affect the stability of the longwall entry roof. Based on this stress analysis, some design and support guidelines for achieving a better stability of longwall entry roof in both the development and mining periods can be proposed.

This dissertation has concentrated on the stress distributions on the roof of longwall entry systems under high horizontal stress. It contains four parts: the basic consideration and initial study; the stress distributions in entry roof during a three-entry-system development; the stress analysis at the T-junctions in longwall mining; and the influences of the interfaces

between the coal seam and the roof/floor and between the roof layers on the stresses in an entry roof.

In the first part, in order to find the more important factors, the effects of the following factors on the stress distributions in entry roof are analyzed: stress angle between maximum horizontal stress and entry direction; stress ratio of the maximum to minimum horizontal stresses; overburden depth; and different types of roof.

Based on the initial study, the influence of the more important factors on the stress distribution in the roof of a three-entry system has been investigated. In this part, the stresses in entry roof have been analyzed. In addition, the roof stress in the crosscuts have been discussed briefly.

In the third part, the stresses at the T-junctions in longwall mining have been analyzed. For a multiple-panel system, the maximum horizontal stress comes both from the mined-out panel side (the gob side) and from the solid coal side. The difference of the stress in the headgate has been discussed for these two loading conditions.

Finally, the interfaces between the coal seam and the roof/floor and those between the roof layers are investigated in the research. The effects of these interfaces on the stresses in entry roof have been discussed in detail. In this case, slip between the coal and the roof/floor, and the roof separations, occur. The stresses in entry roof have changed.

CHAPTER 2

LITERATURE REVIEW

It is recognized that horizontal stresses are primary tectonic in origin and at depths of less than 0.8 km (0.5 mile), they are usually as great or greater than the vertical stresses^{[19]*} (* references are arranged alphabetically). In-situ horizontal stresses have been observed to adversely affect ground control in coal mines, and the effects of high horizontal stresses on coal mine roof stability have also been observed worldwide. Many roof stability problems have been attributed to high horizontal stresses in recent years. Since the late 1970s, Australian and British ground control researchers have taken the lead in developing technology for detecting and controlling horizontal stress^[12, 37]. In Canada, ground stress determination has been carried out in some coal mines, and it is found that the horizontal stress is greater than the vertical one in some areas^[17]. In the western Canada, underground roadways are in worse condition if they are perpendicular to lateral tectonic stress^[21].

In US coal mines, the effect of horizontal stress on coal roof stability was also observed in the past. In 1948, Roley^[34] described a phenomenon called “pressure cutting” in the Illinois mines. During the 1970s and 1980s, many researchers and mining engineers studied ground control problems in coal mines with high horizontal stresses, such as Dahl and Parsons^[10], Agapito, et al^[1], and Blevins^[4, 5]. The US Bureau of Mines has also performed extensive research on the cutter roof and its control^[18, 24]. In 1987, Su and Peng^[38] studied the intrinsic mechanism of cutter roof failures by combining field investigations, laboratory testing, underground instrumentation, and numerical modeling. During the past 15 years, high horizontal stress has become central to the understanding of coal mine ground control.

Generally speaking, the characteristics of failures attributing to high horizontal stresses in longwall mines include:

- (1) Compressive-type roof failures, commonly called “cutter roof”, “guttering”,
thinly-bedded (laminated) rock, a classic cutter roof
develops as a result of the progressive layer-by-layer crushing and buckling of
individual beds.

- (2) Directionality of roof falls. Many horizontal stress fields are distinctly biaxial, with a maximum horizontal stress much greater than the minimum horizontal stress. As a result, entries oriented nearly perpendicular to the maximum horizontal stress suffer greater damage than those oriented parallel to it.
- (3) Headgate roof problems. In the absence of horizontal stress, headgates are usually less troublesome than tailgates because they are subjected to lower vertical stresses. Headgates that are consistently more troublesome are indicative of concentrated horizontal stresses.

2.1 Horizontal Stresses in US Coal Fields

In 1987, Plumb and Cox^[33] summarized the knowledge about the orientation of horizontal stress field in northeastern North America. Sources of their data included hydraulic fracturing stress measurements, borehole “breakouts” or elongations, and centerline fractures in the oriented cores. The measured depth ranged from 457 m to 1,200 m (1,500 to 4,000 ft). The data indicated that the maximum horizontal stresses were along E-NE direction, with some rotation towards E-W direction in the Illinois basin, as shown in Fig. 2-1. Stress measurements conducted in 25 underground coal mines throughout the eastern US confirmed the presence of the E-NE stress field^[27]. Figure 2-2 shows that 67% of the measurements from mines in the Appalachian and Warrior coal basins found the orientation of maximum horizontal stress between N50E and N80E. In the Illinois basin, 75% of the measurements indicated that the stress field is rotated towards E-W direction by about 15⁰. The stress provinces of the U.S. is shown in Fig. 2-3^[42].

Stress measurements confirmed that, in mines located in the eastern United States, the magnitude of the maximum horizontal stresses is typically three times greater than the vertical stresses^[29]. The horizontal stress field is biaxial, with the maximum horizontal stress usually about 40% greater than the minimum.

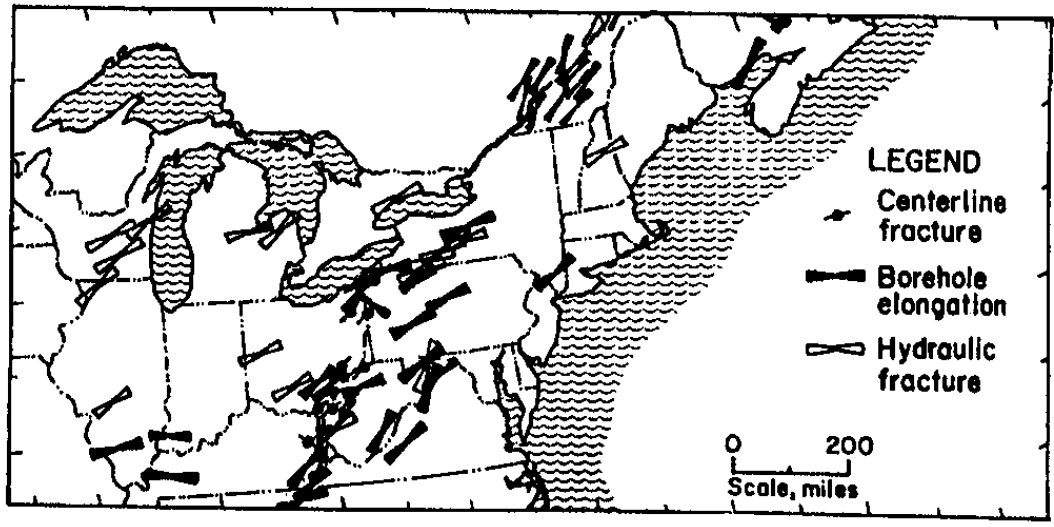


Fig. 2-1 Orientation of the Maximum Horizontal Stress in Deep Boreholes (after Plum and Cox, 1987)

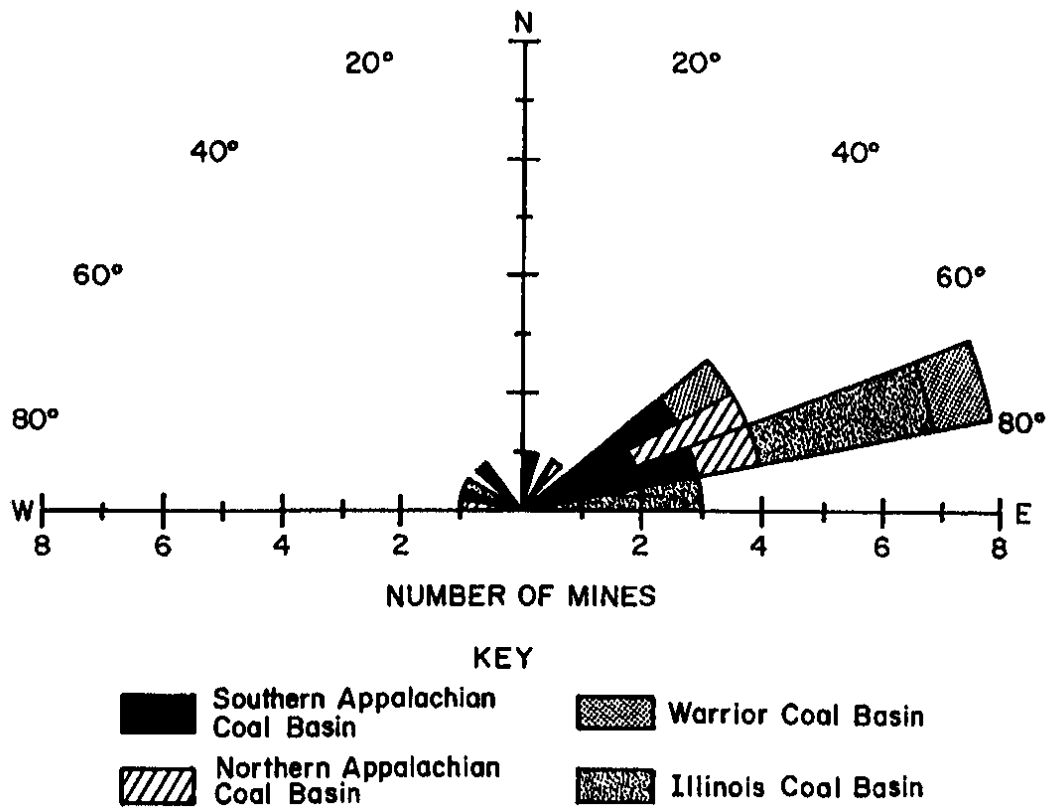


Fig. 2-2 Orientation of the Max. Horizontal Stress Measured In Eastern US Coal Mines (after Mark, 1991)

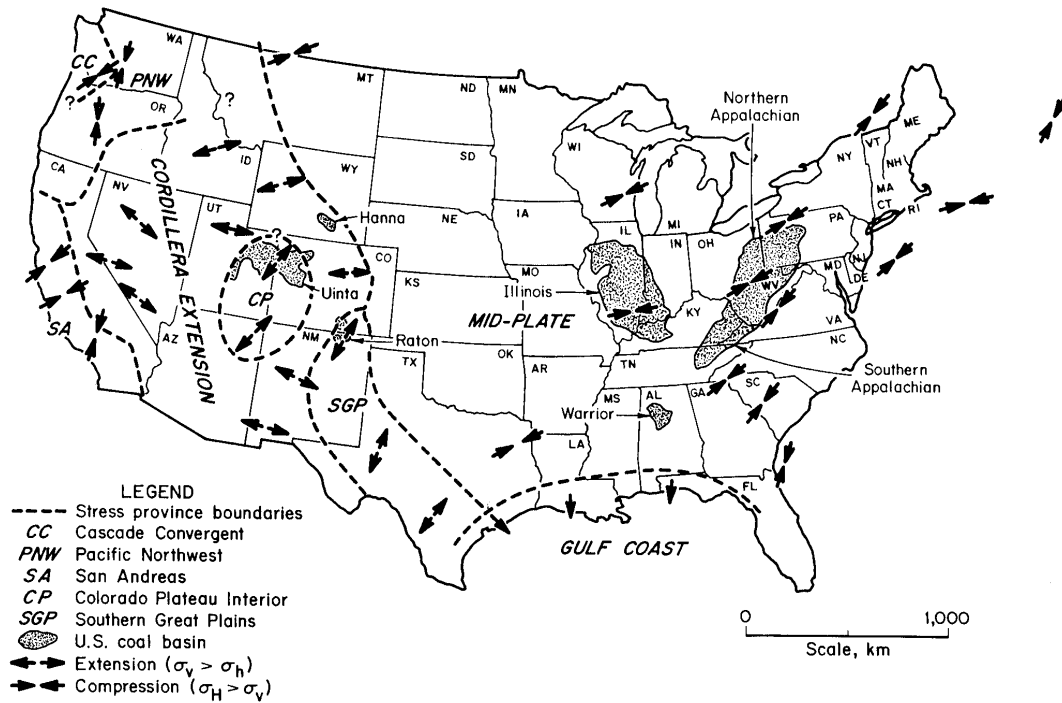


Fig. 2-3 Stress Provinces of the Continental United States (after Zoback and Zoback, 1989)

In-situ horizontal stress measurements were conducted in several northern Appalachian coal mines using a Minifrac system by Su and Hasenfus^[39]. The measurements are shown in Fig. 2-4 and Table 2-1. Table 2-2 shows the horizontal stresses at six West Virginia mines^[31].

All measurements confirm that there are high horizontal stress fields in the eastern US coal fields.

Table 2-1 Results of Minifrac Stress Measurements in Southwestern PA and Northern WV^[39]

Horizontal Stress	Mine 1	Mine 2	Mine 3	Mine 4
Max. Horizontal Stress (psi)	4,580	4,030	5,200	3,000
Min. Horizontal Stress (psi)	3,260	3,400	3,500	1,800
Orientation of Max. Horizontal Stress (azimuth)	90 ⁰	90 ⁰	90 ⁰	75 ⁰
Overburden Depth (ft)	800	800	640	600
Distance above Mine Roof (ft)	23.5	12	18	12

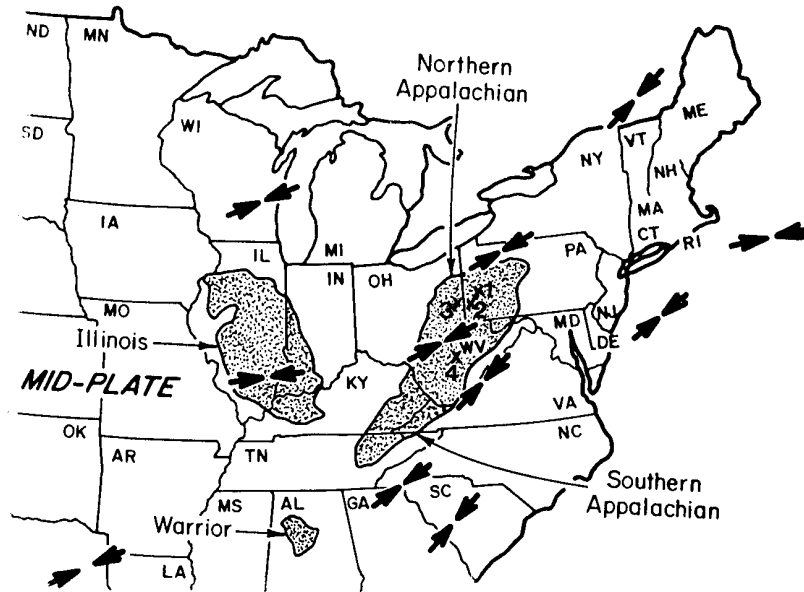


Fig. 2-4 Regional Horizontal Stress Fields and Locations of Mines (after Su and Hasenpus, 1995)

Table 2-2 Horizontal Components of in-situ Stress at Six West Virginia Mines^[31]

Mine	Overburden (ft)	Max. Horizontal Stress (psi)	Min. Horizontal Stress (psi)	Direction of Max. Horizontal Stress	Hole Depth (ft)
Olga	1,250~1,500	3,200	2,300	N60°E	5~13
Bonny	1,140	3,800	3,100	N57°E	15~22
Beckley	830	3,300	2,500	N59°E	10~26
Beckley #1	1,100	3,200	1,900	N75°E	5~15
Beckley #2	1,100	2,300	1,700	N52°E	10~12
Maple Meadow	860	3,400	2,500	N68°E	9~25

2.2 Cutter Roof Failure

Cutter roof failure is a specific type of ground control problem which frequently results in massive roof failure. It is a common occurrence in coal mines of the Northern Appalachian Coal basin. Cutter roof initiates and propagates nearly vertically from one or

both upper corners of an entry and is difficult to control by conventional roof support, as shown in Figs. 2-5 and 2-6.



Fig. 2-5 Typical Cutter Roof Failure at Entry Corner (after Hill, 1984)

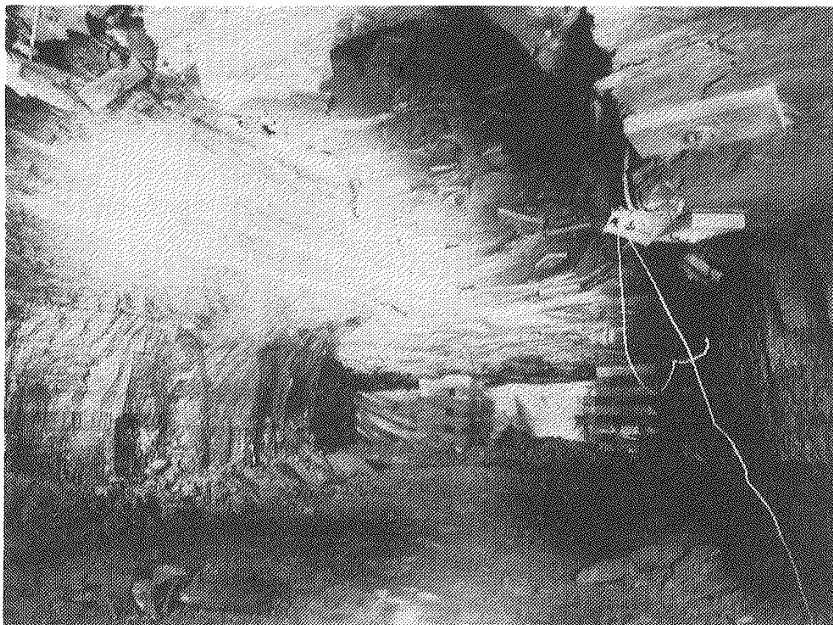


**Fig. 2-6 Remaining Cavity Following Overall Roof Collapse
(Courtesy Bureau of Mines, Pittsburgh Research Center)**

It has been suggested that cutter roof is caused by the shear stress at the entry corners being larger than the shear strength. This high shear stress at the corners results from either a large overburden weight and/or high horizontal stress at the rib. If separations between strata

or a weak bedding plane exist, shear failures that originate at the corners and propagate upward may stop at the first separation of a weak bedding plane. Traditionally, the kind of problem encountered with supporting roof conditions of this nature is that, regardless of the length of roof bolt installed, with time, a massive roof collapse still results, usually to a height equal to the bolt length as shown in Fig. 2-7^[24].

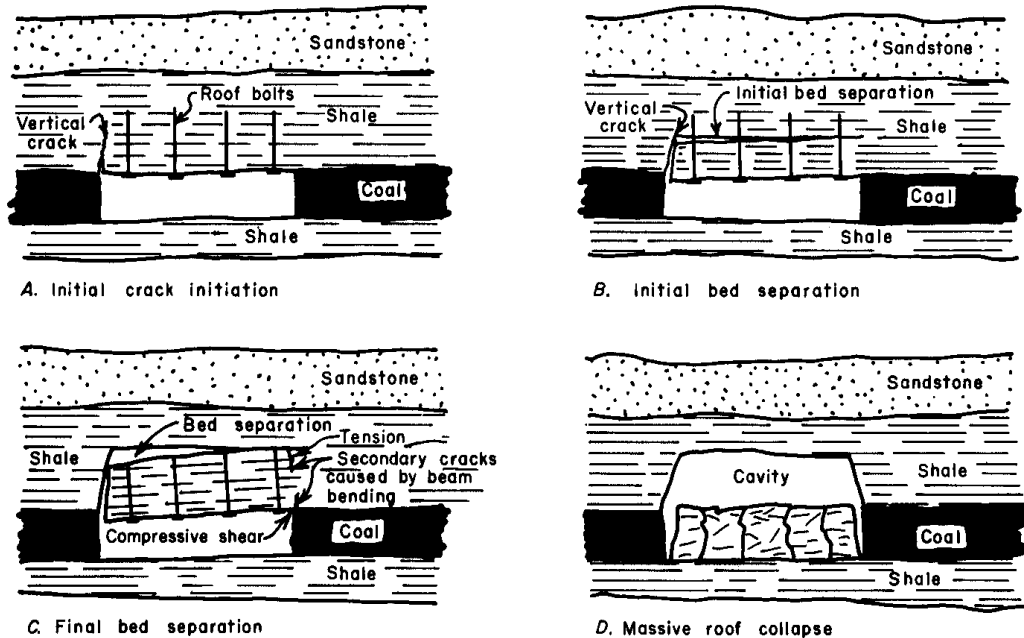


Fig. 2-7 Progressive Sequence of Events Leading to Overall Roof Collapse Resulting from Cutter Roof Failure (after Kripakov, 1982)

2.2.1 In-situ Observations

In many coal mines cutter roof failures have been observed, as described previously. A few representative cases are described here.

Case 1: Roof Problems in BethEnergy's Eighty Four Complex Mine^[25, 30]

Figure 2-8 shows the layout of panels. In the study site, the immediate roof was comprised of thinly laminated shale and coals. The entry width was 16 to 18 ft and the overburden generally varied between 450 and 700 ft. Two types of roof control problems occurred at BethEnergy's Eighty Four Mine in Southwestern Pennsylvania, namely poor roof conditions encountered while advancing submain entries and longwall panel entries and

deterioration and failure of longwall gateroads, principally the tailgate entry. Both of these problems were initiated by high horizontal stresses and weak/laminated roof strata at the problem areas.

Roof control problems during entry development occurred when the faces of the 33 mains entries completely caved. Severe “cutter roof” problems were encountered in the 2 Butt-D development section, the 3 NE submains, and the 2 Left, 3 Left and 4 Left longwall development sections. Figures 2-9 and 2-10 show the cutter roof failures in the entries.

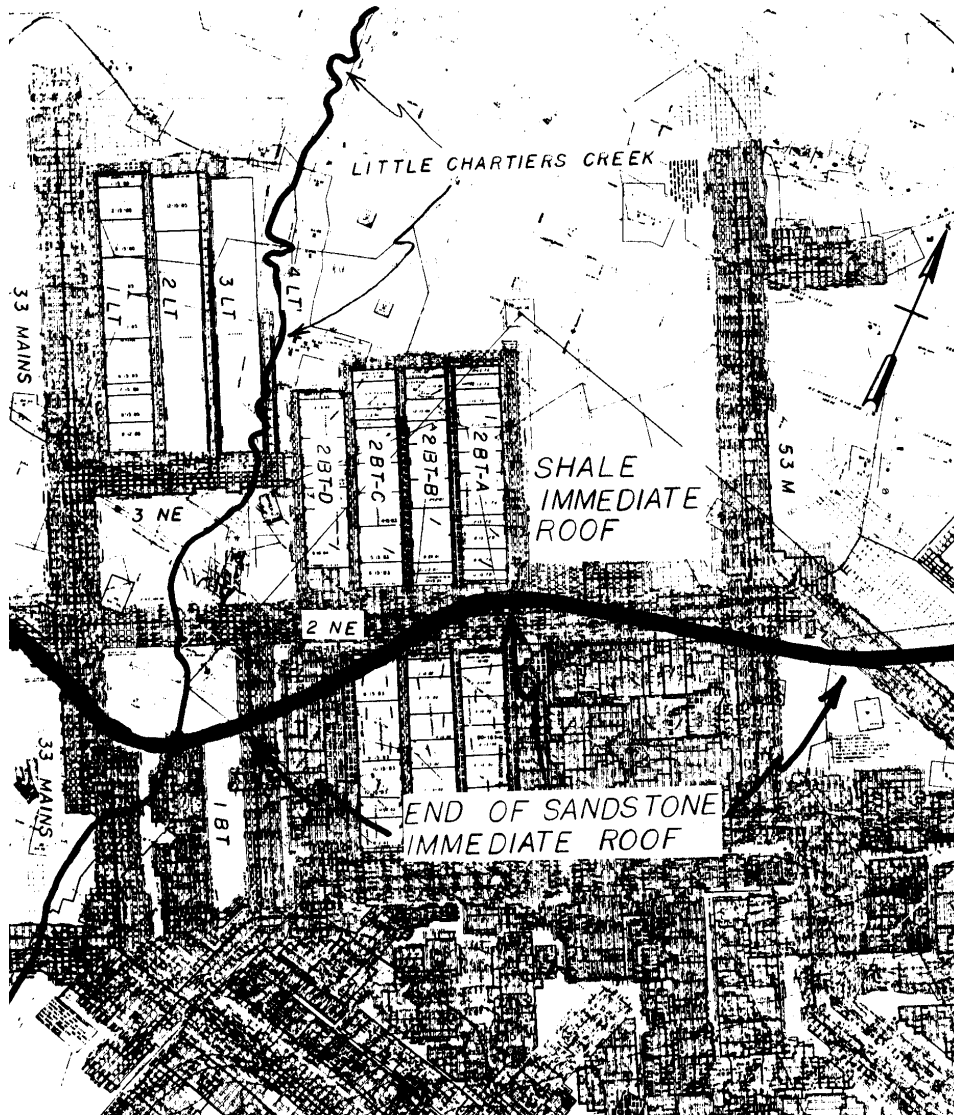


Fig. 2-8 Layout of Study Site in Beth Energy Mines (after Mucho, 1986)

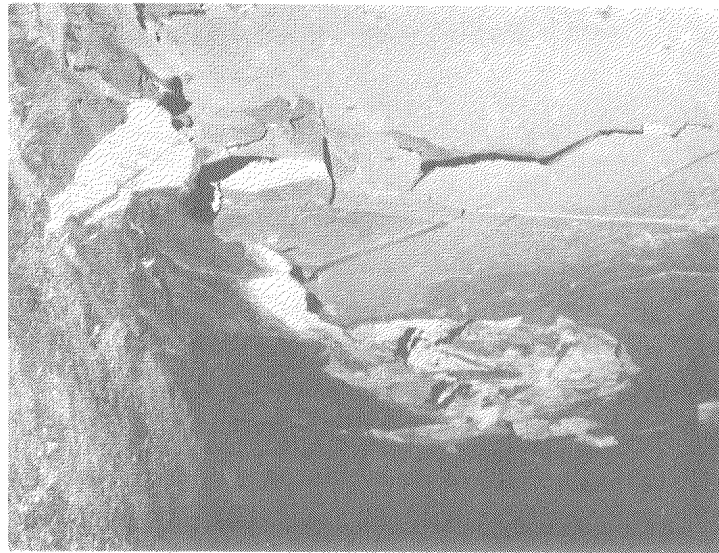


Fig. 2-9 Cutter Roof Develops a Short Distance behind the Face and Follows Entry Advance (after Krupa and Khair, 1991)



Fig. 2-10 Failed Roof Bolt at the Cutter Zone (after Krupa and Khair, 1991)

The second ground control problem was the control of longwall gateroads. The most significant failures occurred in the tailgate entry. At first, no gateroad problems were observed when longwall panels 2 BT-A and 2 BT-B were mined out (Fig. 2-8). However, by the time the third panel (2 BT-C) in the section was mined, it was obvious that stresses were

increasing in the tailgate entry. At the start of the panel 2 BT-D, severe destruction of longwall tailgate entry had occurred. The front abutment pressure acting on the already deteriorated entry caused the tailgate entry to fall despite the fact that additional 30" x 6" x 5" wooden cribs had been installed.

BethEnergy personnel believed that the "cutter roof" problem was caused by the horizontal stresses concentrated under the north-south stream valleys which may also cause a distortion of the stress field. This problem became apparent when weak immediate roof and/or other geological structures were present. The other problem was increasing gateroad loading on successive longwall panels, ultimately resulting in failure.

Case 2: Cutter Roof Failure in West Virginia Coal Mine^[38]

Figure 2-11 shows the longwall projection of a coal mine in West Virginia (Su and Peng, 1987). The immediate roof over most parts of the mine consisted of a layer of gray shale (3~4 ft), overlain by a thick layer of sandstone. Over the portion of the mine where cutter roof failures were observed in longwall development entries, however, the immediate roof was a layer of black shale (3~4 ft) overlain by a layer of gray shale (3~4 ft). Overburden depth was around 800 ft.

Cutter roofs usually occurred in the first and second entries one or two breaks behind the faces, as shown in Fig. 2-12. Once the cutter was initiated, cribs were installed to support the roof. Cutter roofs were also spotted along the entries developed from the bleeders near the northern end of the property.

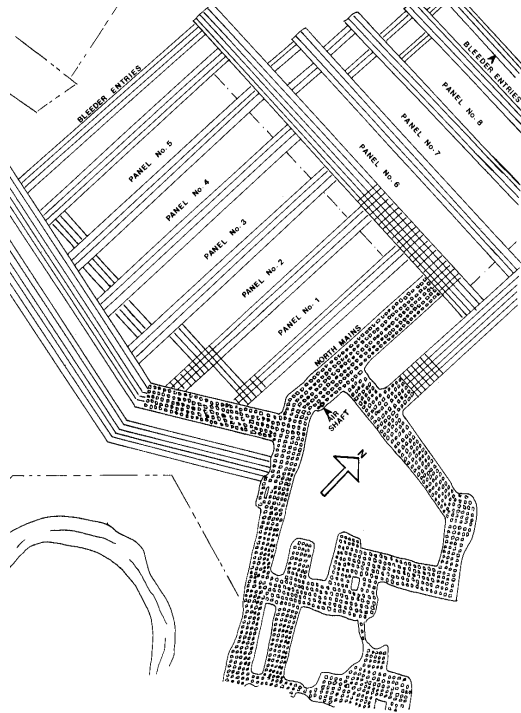


Fig. 2-11 Longwall Projections (after Su and Pang, 1987)

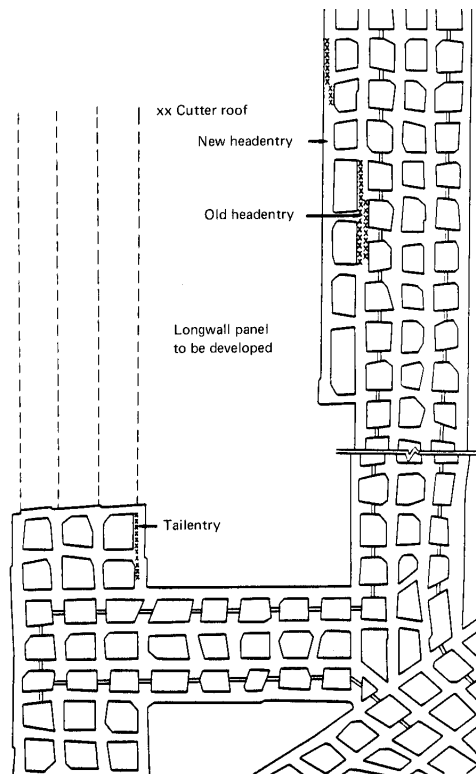


Fig. 2-12 Cuter Roof in Longwall Development Entries (after Su and Peng, 1987)

2.2.2 Causes of Cutter Roof Failure

Many researchers have tried to find the causes of cutter roof. Kripakov^[24] summarized the past explanations about causes of cutter roof failure. They include

- (a) stress caused by depth of cover;
- (b) remnant stresses caused by the tectonic force;
- (c) lateral movement of the strata along the bedding planes;
- (d) variation in the strength of individual rock layer comprising the immediate roof;
- (e) hydraulic pressure;
- (f) gas pressure;
- (g) variation in temperature and humidity; and
- (h) insufficient artificial support.

Recently it has been recognized that the high horizontal stress and weak roof are the main reasons of cutter roof in coal mines. Therefore, horizontal stress and roof properties are main factors considered in the numerical analysis methods.

2.3 Influence of Horizontal Stress on Longwall Mining

In situ horizontal stresses have affected longwall mining throughout the world during both development and longwall retreat. During the development of a panel, the horizontal stress mainly causes roof stability problems, such as cutter roof failure and floor heave. In this period, no stress relief occurs. During longwall retreat, the maximum horizontal stress direction plays a very important role in ground control. For example, in the Pittsburgh coal seam before the advent of longwalls, miners had noticed that cutter roof and “snap top” seemed to occur preferentially in N-S headings. A classic study conducted by Dahl and Parsons^[10] determined that the horizontal stress was responsible for these and other directional phenomena, including floor heave, rib spalling and the formation of tensile cracks.

Based on their pre-longwall mining history and some bad experiences early in the longwall mining, most mines in the Pittsburgh seam have always oriented their longwall panels in nearly E-W direction. At the eight Pittsburgh seam longwall mines, a total of 157 longwall panels have been extracted during the past 20 years. Of these, 58% were oriented between E-

W and N70W. No serious problems attributable to horizontal stress were reported from those panels, except in crosscuts. Another 29% of the panels were oriented between N70W and N60W. Some of those had experienced headgate instability. Only two of the 157 panels had been oriented N-S direction. Both of those experienced conditions so poor that the panels were abandoned before they were completed^[27].

Figures 2-13 shows the different situations of entry roofs in the Inland Steel No.2 Mine when some entries were located along the N-S direction and other were along the E-W direction^[15]. They indicate that entries along the E-W direction (parallel to the maximum horizontal stress) were in good condition while those along the N-S direction were in worse condition.

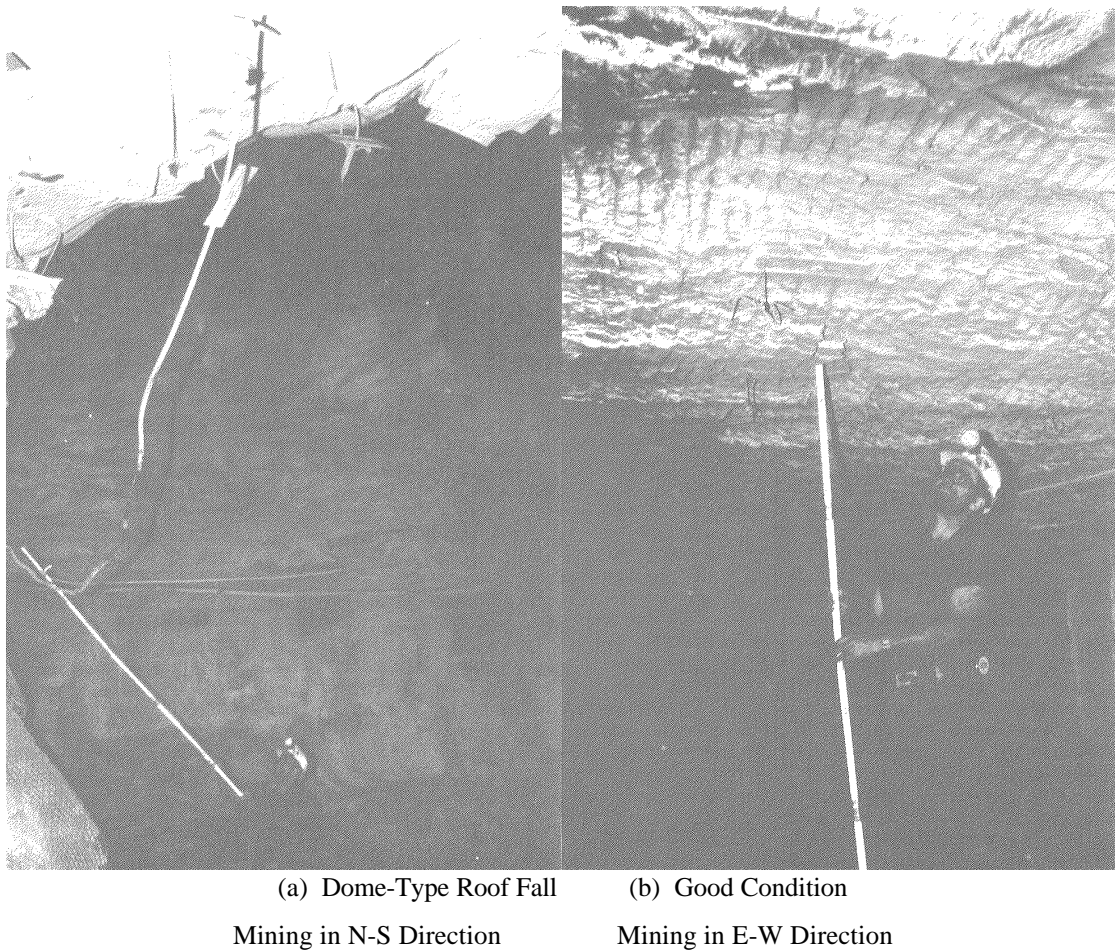


Fig. 2-13 Roof Condition in Different Mining Directions (after Hanna, et al., 1986)

In a multiple-panel system, since the horizontal stress cannot pass through a gob area, zones of stress relief and stress concentration are created, as shown in Fig. 2-14^[28]. Mark et

al^[28] investigated the headgate problems in several coal mines. Figure 2-15 shows the problems in mines A and B. Mines A and B are adjacent Pittsburgh seam longwall mines located in southwestern Pennsylvania. The average overburden is about 700 ft. The immediate roof is composed of typical Pittsburgh seam sequence of coals and laminated shales and the maximum horizontal stress direction is between N70⁰E and E-W. At mine A, the primary longwall ground control problems have been on the headgate. This is due to panel sequencing. At mine B, the current panel sequence is opposite that of mine A, and the headgate experiences stress-relief conditions during longwall retreat. However, the first panel encountered stress concentrations and several major headgate roof falls.

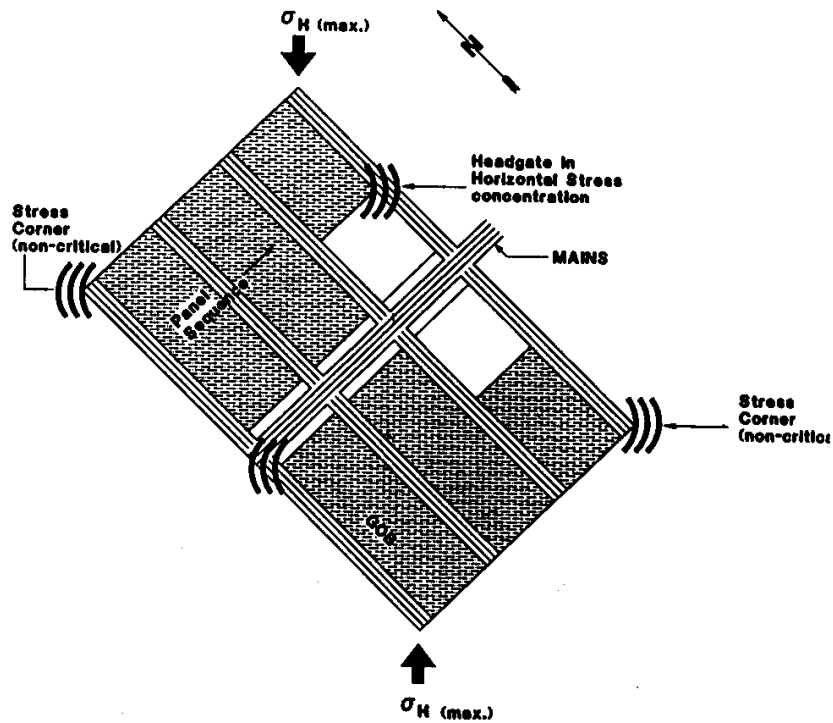


Fig. 2-14 Horizontal Stress Concentration Caused by Retreat Mining (after Mucho and Mark, 1994)

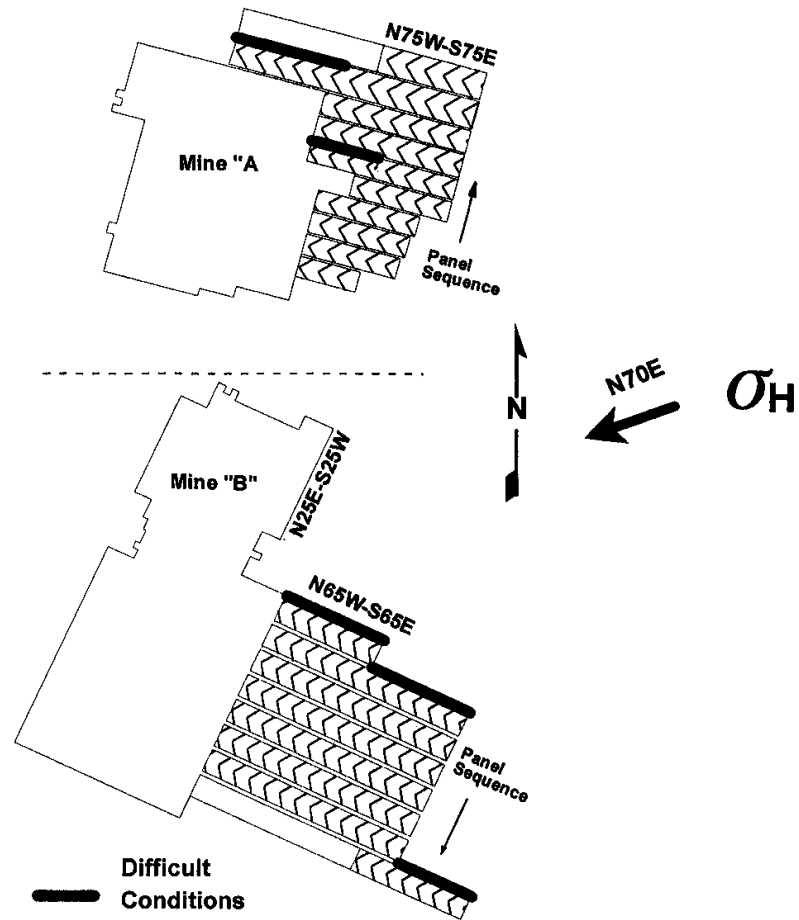


Fig. 2-15 The Study Site in Mines A and B (after Mark, et al., 1998)

In order to research the influence of the angle between the maximum horizontal stress and mining direction on the entry stability in longwall panels, the numerical methods, such as the finite element method and the boundary element method, have been widely used^[2, 27, 41]. Su and Hasenfus^[39] analyzed the stress concentrations in the headgate, using three-dimensional finite element modeling, as shown in Fig. 2-16 and Table 2-3. It was found that the headgate was in worse condition when the angle was $45^{\circ} \sim 90^{\circ}$. Wang and Peng^[41] studied the stress redistributions in the roof of headgate/tailgate entries. In their study, the Von-Mises failure criterion was used. The models used and the results are shown in Fig. 2-17 and Table 2-4, which indicate that the headgate/tailgate entries were in worse conditions when the angle ranged from $67.5^{\circ} \sim 90^{\circ}$ and that the tailgate was worse than the headgate.

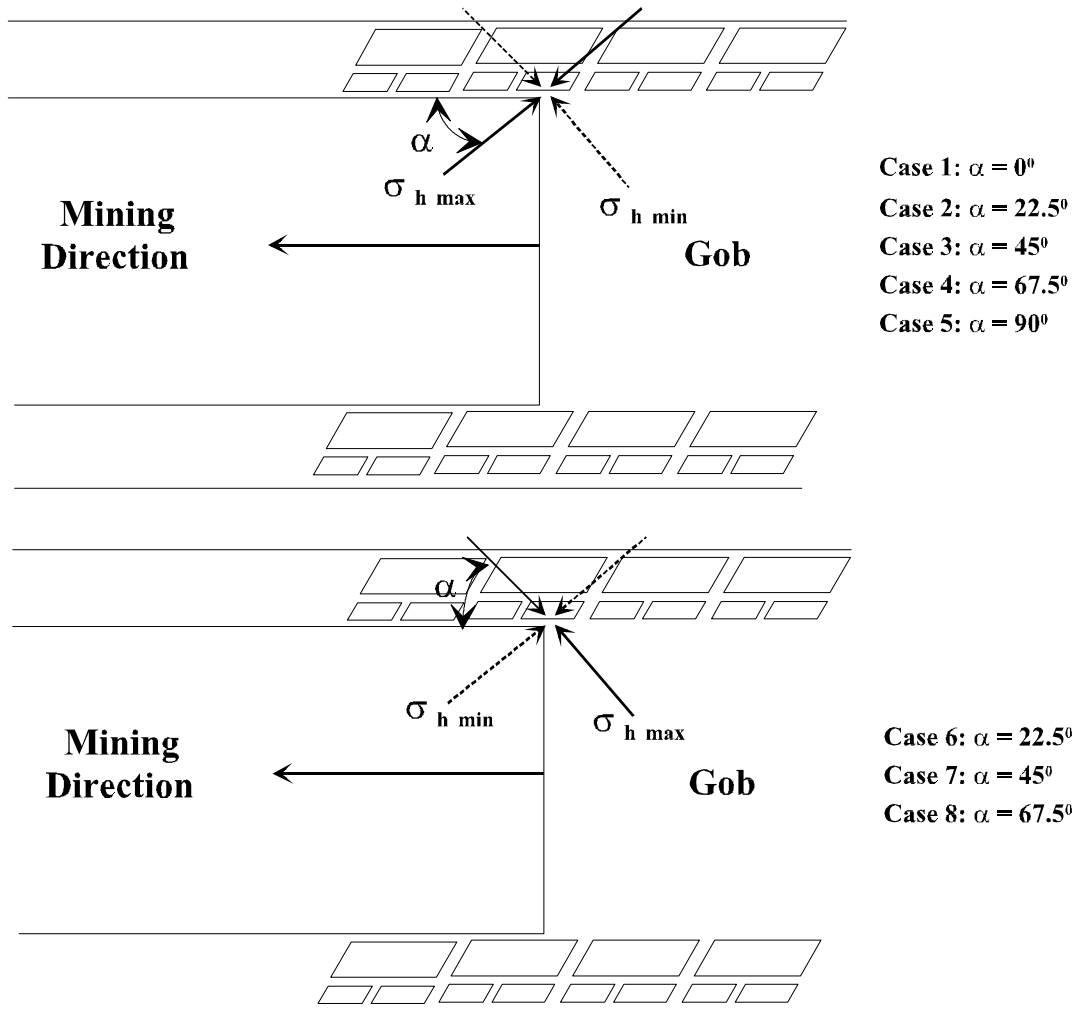


Fig. 2-16 Relative Orientation of Max. Horizontal Stress and Direction of Mining (after Su and Hasenfus, 1995)

Table 2-3 Induced Von-Mises Stress Concentration in the Headgate Roof^[39]

Case	Premining Stress (psi)	Stress After Entry Development (psi)	Stress At Headgate T-Junction (psi)	Case	Premining Stress (psi)	Stress After Entry Development (psi)	Stress At Headgate T-Junction (psi)
1	3,000	6,080	8,610	5	3,000	7,350	10,160
2	3,000	6,480	9,370	6	3,000	6,100	8,330
3	3,000	7,010	10,080	7	3,000	6,500	8,720
4	3,000	7,350	10,400	8	3,000	7,000	9,460

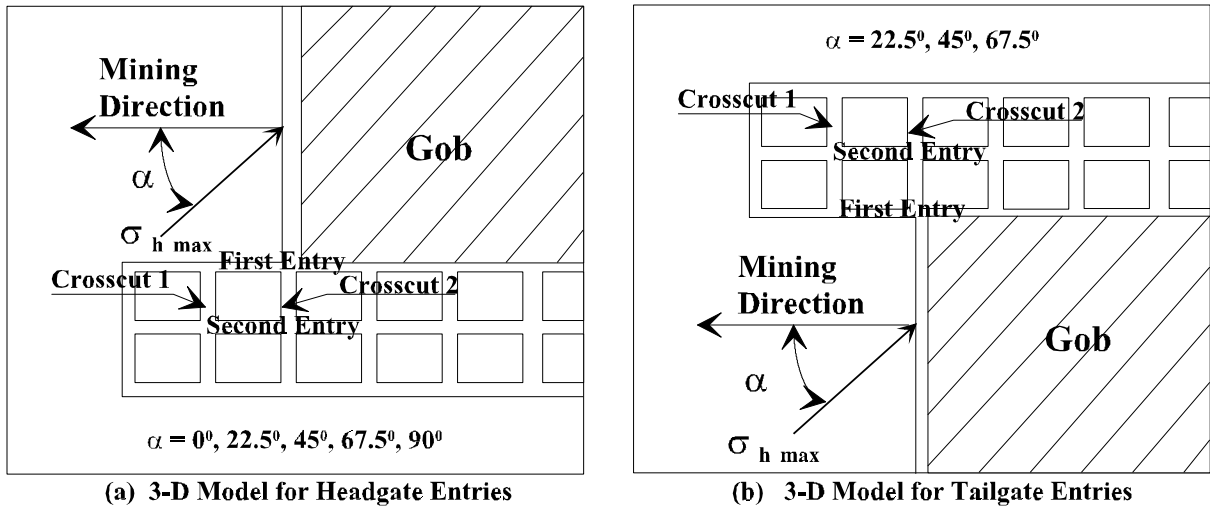


Fig. 2-17 Finite Element Models Used by Peng and Wang

Table 2-4 The Maximum Stress Concentration Factor (SCF)^[41]

α (degree)	First Entry		Second Entry		Crosscut 1		Crosscut 2	
	Headgate	tailgate	Headgate	tailgate	Headgate	tailgate	Headgate	tailgate
0	1.99	1.99	1.72	1.72	2.21	2.21	2.86	2.86
22.5	1.63	2.45	1.85	1.96	1.89	2.18	2.68	2.74
45	2.00	2.71	2.06	2.12	1.55	2.01	2.28	2.68
67.5	2.49	2.97	2.24	2.40	1.42	1.86	1.63	2.37
90	2.89	2.89	2.61	2.61	1.51	1.54	1.80	1.80

SCF = Von-Mises stress during longwall retreating divided by Original Von-Mises stress without mining activities

In addition, the effects of the horizontal stress on the entry stability have been widely studied in Australia. Fig. 2-18 shows a practical example of the percentage of entries suffering shear fracture of the roof strata plotted as a function of the angle at which the entry is driven to the maximum horizontal stress (Gale, 1991)^[13]. In this example, the vertical stress is about 14 MPa, the maximum horizontal stress is 25 MPa, and the minimum horizontal stress is 14 MPa. It indicates that entries driven parallel to the maximum horizontal stress suffer little or no deformation while those driven at angles about 45° suffer an increasingly significant level of deformation. In addition, the location of roof failure is also influenced by

the angle, as shown in Fig. 2-19. When the angle is from 40° to 75° , the roof failure may occur in one rib side. As the angle increases to 80° to 90° , the area of roof deformation locates toward the entry center (Gale, 1991)^[13].

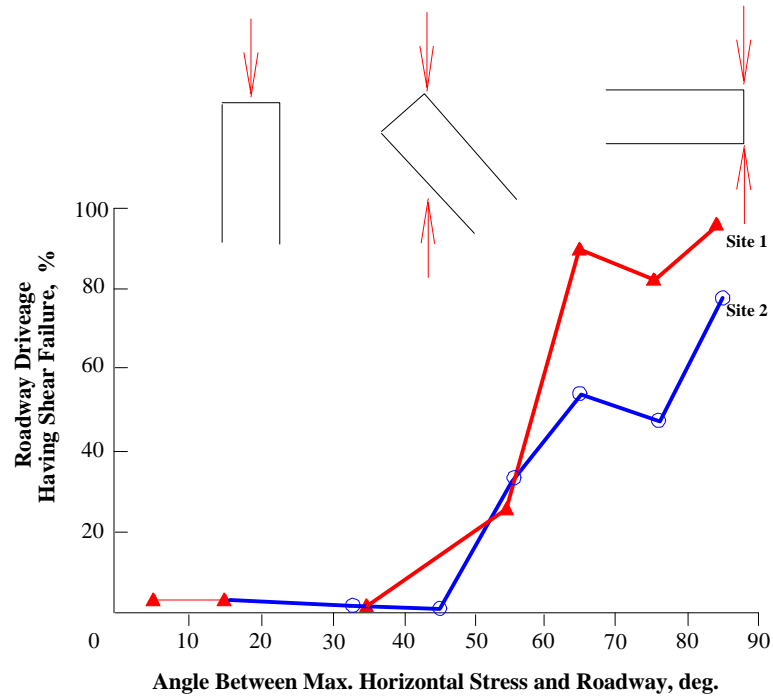


Fig. 2-18 Roof Failure vs. Stress Angle (after W.J. Gale, 1991)

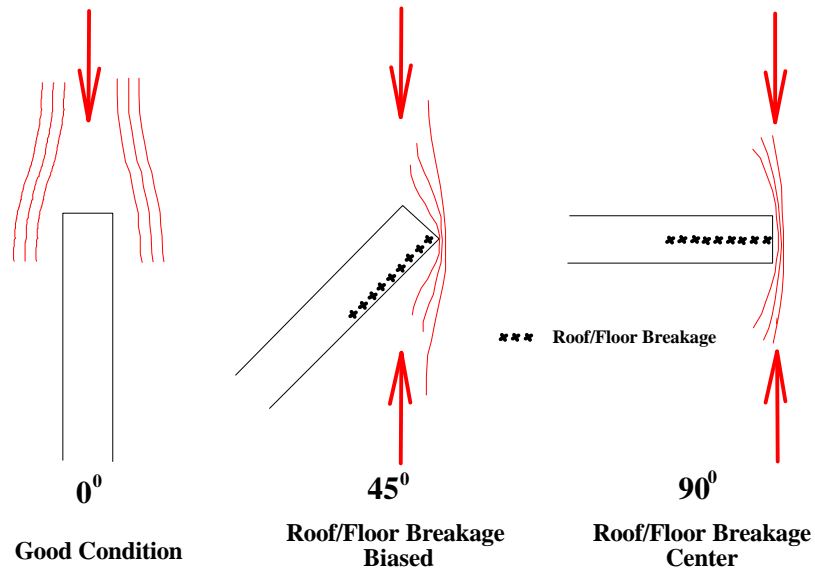


Fig. 2-19 Effect of Horizontal Stress Direction (after W.J. Gale, 1991)

The influence of horizontal stress on the entry stability of longwall panels has been widely studied recently and some control methods have been developed, e.g. the stress-relief method and use of trusses and bolts. Horizontal stress has become central to the understanding of coal mine ground control.

2.4 Remarks on Previous Studies

The literature review presented in the preceding sections indicates that previous researches have mainly focused on the influence of the stress angle between the entry direction and the maximum horizontal stress on the entry stability and that the following areas of interest have not been studied adequately:

- (1) the locations of roof failure;

Field observations have found that the cutter roof failure occurred at different locations and at different time after mining. It occurred both before and after mining. After mining, it sometimes occurred on the right-hand side rib at the face while sometimes on the left-hand side rib. Sometimes it did not occur at the face but some distance outby the face either on the right-side or left-side rib. Sometimes it occurred on the right-side rib and then changed to the left-side rib. Especially, in a multiple-entry system, the locations of the cutter roof failure often change at different parts of the mine.

- (2) the roof stress at the T-junctions in a longwall panel when the adjacent panel is mined out;

In this case, the maximum horizontal stress is either from the mined-out panel side or from the other side. Under these loading conditions, the headgate entries are subjected to different loadings.

- (3) the influence of interface sliding between the coal seam and roof/floor and the influence of the roof separations.

Although it has been recognized that the interface sliding and strata separation influence the roof stability significantly, the research in this aspect has hardly been reported.

In the following chapters, these aspects of the subjects are addressed through a series of parametric studies employing a numerical stress-analysis method.